1 **Measurement report: Brown Carbon Aerosol in Polluted Urban Air of North China Plain:**

2 **Day-night Differences in the Chromophores and Optical Properties**

3 **Yuquan Gong[1,2], Ru-Jin Huang[1,2,3,4], Lu Yang[1,2], Ting Wang[1], Wei Yuan[1,2], Wei Xu[1],**

4 **Wenjuan Cao[1], Yang Wang [5,6], Yongjie Li[7]**

5 [1] State Key Laboratory of Loess and Quaternary Geology, CAS Center for Excellence in

6 Quaternary Science and Global Change, Institute of Earth Environment, Chinese Academy of

7 Sciences, 710061 Xi'an, China

8 [2] University of Chinese Academy of Sciences, Beijing 100049, China

9 [3] Institute of Global Environmental Change, Xi'an Jiaotong University, Xi'an 710049, China

10 [4] Laoshan Laboratory, Qingdao 266061, China

11 [5] School of Geographical Sciences, Hebei Normal University, Shijiazhuang, China

12 [6] State Key Joint Laboratory of Environmental Simulation and Pollution Control, Beijing, China

13 [7] Department of Civil and Environmental Engineering, Faculty of Science and Technology,

14 University of Macau, Taipa, Macau SAR 999078, China

15 Correspondence: E-mail: rujin.huang@ieecas.cn (R.-J.H)

Atmospheric
Chemistry
and Physics
Discussions

16   **Abstract.** Brown carbon (BrC) aerosol is light-absorbing organic carbon that affects radiative

17   forcing and atmospheric photochemistry. The BrC chromophoric composition and its linkage

18   to optical properties at the molecular level, however, are still not well characterized. In this

19   study, we investigate the day-night differences in the chromophoric composition (38 species)

20   and optical properties of water-soluble and water-insoluble BrC fractions (WS-BrC and WIS-

21   BrC) in aerosol samples collected in Shijiazhuang, one of the most polluted cities in China. We

22   found that the light absorption contribution of WS-BrC to total BrC at 365 nm was higher during

23   the day ($62 \pm 8\%$) than during the night ($47 \pm 26\%$), which is in line with the difference in

24   chromophoric polarity between daytime (more polar nitrated aromatics) and nighttime (more

25   less-polar polycyclic aromatic hydrocarbons, PAHs). The high polarity and water solubility of

26   BrC in daytime suggests the enhanced contribution of secondary formation to BrC during the

27   day. There was a decrease of the mass absorption efficiency of BrC from nighttime to daytime

28   (2.88 ± 0.24 vs. 2.58 ± 0.14 for WS-BrC and 1.43 ± 0.83 vs. 1.02 ± 0.49 m^2 g C^{-1} for WIS-BrC,

29   respectively). Large polycyclic aromatic hydrocarbons (PAHs) with 4–6-rings PAHs and

30   nitrophenols contributed to 76.7% of the total light absorption between 300–420 nm at night

31   time, while nitrocatechols and 2–3-ring oxygenated PAHs accounted for 52.6% of the total light

32   absorption at day. The total mass concentrations of the identified chromophores showed larger

33   day-night difference during the low-pollution period (day-to-night ratio of 4.3) than during the

34   high-pollution period (day-to-night ratio of 1.8). The large day-night difference in BrC

35   composition and absorption, therefore, should be considered when estimating the sources,

36   atmospheric processes and impacts of BrC.

Atmospheric
Chemistry
and Physics
Discussions

1 Introduction

37

38   Light-absorbing organic carbon aerosols, also termed brown carbon (BrC) aerosol, are

39 ubiquitous in the atmosphere (Iinuma et al., 2010; Yuan et al., 2016; Huang et al., 2021).

40 Growing evidence has shown that BrC can reduce atmospheric visibility, affect atmospheric

41 photochemistry, and change regional and global radiation balance (Kirchstetter et al., 2004;

42 Laskin et al., 2015; Hammer et al., 2016). Besides, some components in BrC, such as polycyclic

43 aromatic hydrocarbons (PAHs) are highly toxic and carcinogenic, which can adversely impact

44 human health (Alcanzare, 2006; Zhang et al., 2009; Huang et al., 2014). The extent of these

45 effects is closely related to the optical properties and chemical composition of BrC, which are

46 still not well understood.

47   BrC is often classified into water-soluble (WS-BrC) and water-insoluble (WIS-BrC)

48 fractions because these two fractions are largely different in chemical composition and light

49 absorption. For example, abundant nitrophenols were detected in WS-BrC, while polycyclic

50 aromatic hydrocarbons (PAHs) were the main component of WIS-BrC (Huang et al., 2018;

51 Huang et al., 2020). The difference in BrC chemical composition is associated with the emission

52 sources. For example, methyl nitrocatechols are specific to biomass burning, while PAHs are

53 mainly emitted by fossil fuel combustion (Kitanovski et al., 2012; Dat and Chang, 2017).

54 Atmospheric oxidation can further complicate the BrC chromophores dynamically, leading to

55 light-absorbing enhancement or bleaching. For example, Li et al. (2020) reported that the mass

56 absorption efficient (MAE) of some nitroaromatic compounds (e.g., nitrocatechols) from the

57 biomass burning can enhance about 2−3 times by oxidation to generate secondary

58 chromophores. Yet, prolonged photo-oxidation reactions (exposure to sunlight for few hours)

59 of these nitroaromatic can generate small fragment molecules (e.g., malonic acid, glyoxylic

60 acid) and rapidly reduce the particle absorption (Hems and Abbatt, 2018; Wang et al., 2019b;

61 Li et al., 2020). The complexity in composition and sources, as well as the dynamics in their

62 atmospheric processing limit our understanding in BrC chromophores and their links to light

63 absorption.

64   In recent years, a growing number of studies have investigated the chromophore

65 composition of BrC and found that nitro-phenols, low ring acids/alcohols, PAHs and carbonyl

66 oxygenated PAHs (OPAHs) were the major chromophores in BrC (Teich et al., 2017; Yuan et

67 al., 2020; Huang et al., 2020). Some chromophores in BrC can be generated from both primary

68 emission and secondary formation. For example, 4-nitrophenol and 4-nitrocatechol can be

69 emitted directly from biomass burning and can also be generated through photo-oxidation

70 reactions (Kitanovski et al., 2012; Yuan et al., 2020). The differences in emission sources or

71 atmospheric oxidation conditions have a significant effect on the chemical composition of BrC

72 chromophores. Previous studies mainly focused on seasonal variations of BrC chromophores

73 (Wang et al., 2018; Kasthuriarachchi et al., 2020; Yuan et al., 2021), and the diurnal variation

74 of WS-BrC in fluorescence and inorganic fractions (Deng et al., 2022; Zhan et al., 2022),

75 however, the research of BrC chemical composition on day-night differences is scarce. In this

76 study, the optical properties and chemical composition of the WS-BrC and WIS-BrC in daytime

77 and nighttime were measured with a high-performance liquid chromatography–photodiode

78 array–high-resolution mass spectrometry platform (HPLC-PDA-HRMS) in $PM_{2.5}$ samples

79 collected in Shijiazhuang, one of the most polluted cities in the Beijing-Tianjin-Hebei region.

80 Besides, the relationship between the concentration and light-absorbing contributions of the

81 BrC subgroups was analyzed. The object of this study is to investigate the day-night differences

82 in the optical properties and chromophore composition of BrC and to explore the effect of

83 primary emissions and atmospheric processes on the light absorption and chemical composition

84 of BrC.

85 **2   Experimental**

86 **2.1 Sample collection.**

87   Day and night $PM_{2.5}$ samples were collected on the quartz-fiber filters (8*10 in., Whatman,

88 QM-A; filters prebaked at 750 °C, over 3 h) through a high-volume air sampler (Hi-Vol $PM_{2.5}$

89 sampler, Tisch, the velocity of flow ~1.03 m^3 min^{-1}, Cleveland, OH) from 17 January to 13

90 February 2014. Daytime samples were collected from 08:30 to 18:30 (~10 hours), and nighttime

91 samples are collected from 18:30 to the next day at 8:30 (~14 hours). After collection, the

92 samples were stored in a freezer (-20°C) until analysis. The sampling site was located on the

93 rooftop of a building (~15 m above ground) in the Institute of Genetics and Developmental

94   Biology, Chinese Academy of Sciences (38.2° N, 114.3° E), which is surrounded by a

95   residential–business mixed zone.

96   **2.2 Light Absorption Measurement.**

97   A portion filter (about 0.526 cm^2 punch) was taken from collected samples and sonicated

98   for 30 min in 10 mL of ultrapure water (>18.2 MΩ) or methanol (J. T. Baker, HPLC grade), and

99   then the extracts WS-BrC and methanol soluble BrC (MS-BrC) were obtained. The extracts

100   were filtered with a 0.45 μm PVDF (water soluble) or PTFE (water insoluble) pore syringe

101   filter to remove insoluble substances. The light absorption spectra of the filtrate were tested

102   using a UV-VIS spectrophotometer (Ocean Optics) over the range from 250 nm to 700 nm,

103   equipped with a liquid waveguide capillary cell (LWCC-3100, World Precision Instruments,

104   Sarasota, FL, USA), following the method of Hecobian et al. (2010). To ensure reliable

105   absorbance measurements (Absorbance between 0.2 to 0.8 M m^{-1} at 300nm in this study), the

106   filtrate was diluted with appropriate folds before absorption spectra measurements. In this study,

107   the light-absorbing of WIS-BrC is obtained by MS-BrC minus WS-BrC. The light absorption

108   coefficient (Abs) and absorption data were calculated following the equation:

109    $$Abs_\lambda = (A_\lambda - A_{700}) \frac{V_l}{V_b \times l} \times \ln(10)$$

110   where Abs$_\lambda$ (M m^{-1}) represents the sample absorption coefficient at wavelength of λ; A$_\lambda$ is the

111   absorbance recorded (Random wavelength); A$_{700}$ for explaining baseline drift as the reference

112   during data analysis. V$_l$ (ml) is the total volume of solvent (water or methanol) used to extract

113   the quartz-fiber filters; V$_b$ (m^3) represents the volume of through the filter sample of the air; l

114   (0.94 m) is the optical path length of UV-VIS spectrophotometer and ln (10) is the absorption

115   coefficient with base-e, which is the natural logarithm by using the logarithm conversion with

116   the base-10.

117   About the mass absorption efficiency (MAE) of the filter extracts at wavelength of λ can be

118   defined as:

119    $$MAE_\lambda = Abs_\lambda / C_{OM}$$

120   where C$_{OM}$ (μg m^{-3}) stands for the concentration of water-soluble organic carbon (WSOC) or

121   methanol extracts methanol-soluble organic carbon (MSOC). The concentrations of WSOC

122   were measured with a TOC-TN analyzer (TOC-L, Shimadzu, Japan). The concentration of OC

123   was measured by a thermal-optical carbon analyzer (DRI, Model 2001) with the IMPROVE A

124   protocol (Chow et al., 2011). Note that MSOC is usually replaced with OC because previous

125   studies have shown that methanol has a high extraction efficiency (~90%) for OC. But it is

126   difficult to completely extract the OC by methanol (Chen and Bond, 2010; Cheng et al., 2016;

127   Xie et al., 2019). Here, WISOC is obtained by MSOC minus WSOC.

128   The wavelength dependence that the light absorption chromophore of solution can be

129   characterized by this equation:

130   $$Abs_\lambda = K \cdot \lambda^{-AAE}$$

131   where K is the fitting parameter of the extracts which is constant related to the chromophoric

132   concentration; AAE is known as the absorption Ångström exponent, which depends on the

133   types of chromophores in the solution. In this study, AAE was calculated by linear regression

134   of $\log_{10} Abs_\lambda$ versus $\log10_\lambda$ at 300–400 nm.

135   The MAE of standards samples ($MAE_{S, \lambda}$), e.g., 4-nitrocatechol and 4-nitrophenol, in the

136   water or methanol solvent at a wavelength of λ were calculated as the Laskin et al. (2015)

137   $$MAE_{S,\lambda} = \frac{A_\lambda - A_{700}}{l \times C} \ln(10)$$

138   where C ($\mu g\ mL^{-1}$) is the concentration of the standards in the extracts.

139   **2.3 BrC Chemical composition analysis.**

140   The main chromophores in WS-BrC and WIS-BrC were identified by the HPLC-PDA-

141   HRMS platform (Thermo Electron, Inc.), and the details are presented in our previous study

142   (Huang et al., 2020). Firstly, the filter samples (3.5~48.3 cm^2) were ultrasonically extracted

143   with 6 mL of the ultrapure water for 30 min and repeated two times. The extracts were filtered

144   through a PVDF filter (0.45 μm) to remove insoluble materials. Then the solution was subjected

145   to an SPE cartridge (Oasis HLB, USA) to remove water-soluble inorganic salt ions. On the

146   other hand, the residual filters were dried and the WIS-BrC fractions were further extracted two

147   times with 6 mL of methanol for 30 min. to extract the WIS-BrC fractions. Afterward, the

148   extracts of WS-BrC and WIS-BrC chromophores were dried with a gentle stream of nitrogen

149   and then redissolved in 150 μl of ultrapure water and methanol.

150   The BrC factions were analyzed by an HPLC-PDA-HRMS platform (including the Dionex

151   UltiMate system and the high-resolution Q Exactive Plus hybrid quadrupole-Orbitrap mass

152   spectrometer). Here, the extracts were loaded onto a Thermo Accucore RP-MS column by the

153   binary solvent with an aqueous solution containing 0.1% formic acid and methanol solution

154   containing 0.1% formic acid as mobile phases L_1 and L_2, eluting at a flow rate of 0.3 mL min^{-}

155   ^{1}. The process of gradient elution here was set as follows: firstly, aggrandize linearly the

156   concentration of L_2 from 15% to 30% in the preliminary 15 minutes, and then linearly increased

157   to 90% from 15 to 45minutes, held at 90% from 45 to 50 minutes, afterward decreased to 15%

158   from 50 to 52 minutes and held there for 60 minutes. The Q Exactive Plus hybrid quadrupole-

159   Orbitrap mass spectrometer, negative/positive mode ESI (-)/ESI (+) for details usage and data

160   processing can refer to in the article by Huang et al. (2020) and Liu et al. (2016). Briefly,

161   HPLC/PDA/HRMS platform was employed in ESI (-) and ESI (+) mode to acquire BrC

162   fractions that mass range from m/z 100 to 800. Strongly polar aromatic hydrocarbons like

163   nitrophenol and carboxylic acid are preferentially ionized in ESI (-) mode, conversely, ESI (+)

164   mode is helpful to detect OPAHs (Oxygenated PAHs) and PAHs fractions (Lin et al., 2017).

165   The absorption spectra of chromophores were measured by a PDA detector in the wavelength

166   range of 190-700 nm. In this study, 38 BrC components (20 WS-BrC and 18 WIS-BrC species)

167   were detected by mass spectrometry and PDA spectroscopy (see Table S1). Mass data processed

168   by the Xcalibur 4.0 software which the parameter of molecular mass set in ± 3 ppm and

169   maximum numbers of atoms for the formula calculator set as 30 ^{12}C, 60 ^{1}H, 15 ^{16}O, 3 ^{14}N, 1 ^{32}S,

170   1 ^{23}Na. The results of this study were corrected by a blank.

3   Results and discussion

3.1 Optical properties of BrC during the day and night.

173   Figure 1 (a) shows the average absorption spectra of WS-BrC and WIS-BrC at the

174   wavelength range between 300 and 500 nm during the day and the night. It can be seen that the

175   light absorption of both WS-BrC and WIS-BrC sharply increased toward the short wavelength.

176   The average absorbance of WS-BrC is 46.04 ± 35.92 M m^{-1} (at 365 nm) during the day that is

177   much higher than the night (27.90 ± 24.80 M m^{-1}). However, the light absorption of WIS-BrC

178   at 365 nm is lower during the night (35.68 ± 35.50 Mm^{-1}) than during the day (40.89 ± 23.42

179   M m^{-1}). The day-night differences of light absorption of WS-BrC and WIS-BrC indicates the

Atmospheric
Chemistry
and Physics
Discussions
Open Access
EGU

180   difference in water solubility and polarity of the chromophores. The average AAE of WS-BrC

181   (AAE_{WS-BrC}) and WIS-BrC ($AAE_{WIS-BrC}$) during the day are 5.10 ± 0.28 and 6.36 ± 0.45,

182   respectively, which are lower than those of the night (5.51 ± 0.40 and 6.97 ± 0.80, respectively).

183   Note that both during the day and night the AAE_{WS-BrC} is lower than $AAE_{WIS-BrC}$, which is

184   different from findings in previous studies (see Table S2). For example, Huang et al. (2020)

185   found that the AAE_{WS-BrC} was higher (8.2 ± 1.0 and 8.2 ± 1.0 in Beijing and Xi'an, respectively)

186   than that of $AAE_{WIS-BrC}$ (5.7 ± 0.2 and 5.4 ± 0.2 in Beijing and Xi'an, respectively). Besides,

187   MAE_{365} of WS-BrC are 2.0- and 2.5-fold of WIS-BrC during the day (2.88 ± 0.24 vs. $1.43 \pm$

188   $0.83 \ m^2 \ g \ C^{-1}$) and night (2.58 ± 0.14 vs. $1.02 \pm 0.49 \ m^2 \ g \ C^{-1}$), respectively, which is opposed

189   to the results of previous studies. For example, the MAE_{365} of WS-BrC are 0.7- and 0.5-fold of

190   WIS-BrC in winter of Beijing (1.22 ± 0.11 vs. $1.66 \pm 0.48 \ m^2 \ g \ C^{-1}$) (Chen and Bond, 2010)

191   and Xi'an (1.00 ± 0.18 vs. $1.82 \pm 1.06 \ m^2 \ g \ C^{-1}$) (Li et al., 2020), respectively. This result

192   indicates that the chemical composition of BrC in the most polluted city, Shijiazhuang, is

193   different from other urban areas on primary sources and secondary aging process. However,

194   both WS-BrC and WIS-BrC have higher MAE_{365} and average AAE values during the day than

195   the night. This suggests that the day-night differences of AAE and MAE_{365} of BrC fractions are

196   likely associated with the different primary emissions and atmospheric aging processes (Cheng

197   et al., 2016; Wang et al., 2019a; Wang et al., 2020). For example, the AAE and MAE_{365} of BrC

198   emitted from biomass burning (AAE ~7.31, and MAE_{365} ~1.01 $m^2 \ g \ C^{-1}$, respectively) (Siemens

199   et al., 2022) showed large differences with that from vehicle emissions (AAE ~10.5, and

200   MAE_{365} ~0.32 $m^2 \ g \ C^{-1}$) (Xue et al., 2018). Besides, photochemical oxidation of fresh BrC from

201   coal combustion resulted in considerable changes in AAE and MAE_{365}, e.g., the AAE and

202   MAE_{365} of fresh coal combustion emission are 7.2 and $0.84 \pm 0.54 \ m^2 \ g \ C^{-1}$, much higher than

203   those in aged samples (6.4 and $0.14 \pm 0.08 \ m^2 \ g \ C^{-1}$, respectively) (Ni et al., 2021).

204   Figure 1 (b) shows the light absorption contributions of WS-BrC and WIS-BrC to total

205   BrC over the wavelength range of 300–500 nm. It is obvious that the absorption contribution

206   of WS-BrC is increased from 53.8% at 300 nm to 87.4% at 500 nm during the day, and from

207   38.4% to 61.5% during the night. The higher absorption contributions of WS-BrC at longer

208   wavelengths during the day compared to that of the night may be related to photo-oxidation

Atmospheric
Chemistry
and Physics
Discussions

Open Access

EGU

209   reaction in day time (Wang et al., 2019b; Chen et al., 2021). The absorption contribution of

210   WS-BrC accounts for $62 \pm 8\%$ to total BrC absorption at 365 nm during the day, but only $47 \pm$

211   8% during the night. The large difference in BrC light absorption between samples from the

212   day and those from the night observed in this study is comparable with previous studies (Shen

213   et al., 2019; Li et al., 2020), and indicates the significant day-night difference in chemical

214   composition.

215   **3.2 Composition and absorption contribution of BrC during day and night**.

216   In total, 38 major chromophores were quantified in WS-BrC and WIS-BrC with HPLC-

217   PDA-HRMS analysis. According to the characteristics of the molecular structures and

218   absorption spectra, these chromophores are divided into ten subgroups, including two

219   quinolines, four nitrocatechols, six nitrophenols, four aromatic alcohols/acids, four 2–3-ring

220   OPAHs, three 4-ring OPAHs, two 3-ring PAHs, four 4-ring PAHs, five 5-ring PAHs, and four

221   6-ring PAHs. Detailed information about these chromophores is listed in Table S3. Figure 2

222   shows the chemical composition of the identified BrC components during the day and night.

223   The total concentration of these chromophores during the day (169.8 ng/m^3) is similar to that

224   at night (171.8 ng/m^3), and the chemical composition of the BrC subgroups is clearly different

225   between the day and night. For example, nitrocatechols, aromatic alcohols/acids and 2–3-rings

226   OPAHs are the major contributors to the total mass concentration of identified BrC

227   chromophores during the day (accounting for 23.3%, 22.3%, and 16.6%, respectively). These

228   BrC chromophores, however, are the minor components during the night (accounting for 12.1%

229   and 15.6%, and 6.9%, respectively). This result indicates the enhanced formation of these

230   chromophores during the day. On the contrary, the relative contributions of nitrophenols and 4–

231   6-ring PAHs are much lower during the day (15.3% and 15.2%, respectively) than those during

232   the night (35.8% and 24.0%, respectively). During the night, 4-nitrophenol (4NP) contributes

233   24.4% of the total concentration, followed by 2-methyl-4-nitrophenol, fluoranthene, and

234   chrysene (2M4NP 4.7%, FLU 4.6%, CHR 4.6%, respectively). The higher contributions of

235   nitrophenols and 4–6-rings PAHs at night are likely caused by enhanced primary emissions (Lin

236   et al., 2020; Chen et al., 2021). Our previous study has found that the emitted organic aerosols

237   from coal combustion had a clearly increase at midnight in Shijiazhuang (Huang et al., 2019;

Atmospheric
Chemistry
and Physics
Discussions
Open Access
EGU

238   Lin et al., 2020). Thus, the large contribute of nitrophenols and 4–6-rings PAHs to total mass

239   concentration at night that may be impacted by emissions from the coal combustion.

240   To investigate the source of the BrC chromophores, the mass concentrations (these

241   concentrations of chromophores are OC normalized) of the day and night were compared. The

242   day-to-night ratios of identified BrC compounds in mass concentrations is shown in Figure 3.

243   It can be seen that the average day-to-night ratios of WS-BrC chromophores are 4.87 for

244   quinolines, 3.49 for 2–3-ring OPAHs, 3.47 for nitrocatechols, 0.48 for nitrophenols, and 2.53

245   for aromatic alcohols/acids, respectively. Previous studies have found that quinolines are

246   important products of fossil fuel combustion, and were used as tracers of the vehicular exhaust

247   (Banerjee and Zare, 2015; Xue et al., 2018; Lyu et al., 2019). Thus, the higher day-to-night ratio

248   of quinolines may be due to increased primary emissions from vehicles during the day. Nitro-

249   phenols and vanillin are typical biomass burning tracers for atmospheric aerosols (Harrison et

250   al., 2005; Scaramboni et al., 2015; Huang et al., 2021). Previous studies have identified

251   econdary formation as an important source of phthalic acid (PA) and methyl-nitrocatechols

252   (Chow et al., 2015; Zhang and Hatakeyama, 2016; Liu et al., 2017). In this study, vanillin,

253   phthalic acid, and three methyl-nitrocatechols (including 4M5NC, 3M6NC, and 3M5NC)

254   isomers have high day-to-night ratios (4.16, 3.75 and 3.28, respectively). The high day-to-night

255   ratios of these BrC chromophores suggest that biomass burning and secondary formation likely

256   play important roles in the daytime source of BrC.

257   However, the average day-to-night ratio (~0.48) of nitrophenols is smaller than one. The

258   day-to-night ratio of nitrophenols is similar to values in previous studies (Yuan et al., 2016;

259   Schnitzler and Abbatt, 2018). Besides, previous studies found that emissions from residential

260   coal-fired heating are significant sources of nitrophenols (Wang et al., 2018; Lu et al., 2019).

261   This suggests that coal combustion emissions have important effect on the nocturnal

262   concentration of nitrophenols. Compared with the WS-BrC chromophores (the day-to-night

263   ratio > 2.53), the day-to-night ratios of the WIS-BrC chromophores approach or below one,

264   with average ratios of 1.46 for 3-ring PAHs, 1.34 for 4-ring OPAHs, 0.74 for 4-ring PAHs, 0.91

265   for 5-ring PAHs, and 0.79 for 6-ring PAHs, respectively. A number of studies showed that coal

266   combustion was the dominant source of PAHs (Wang et al., 2018; Xie et al., 2019; Yuan et al.,

267 2020). Thus, the local emissions may be responsible for the majority of 4–6-rings PAHs during

268 the night.

269   Figure S1 (see Supplemental Information) shows the light absorption contributions of the

270 BrC subgroups to total BrC subgroups in the wavelength range between 300 and 420 nm (the

271 absorptions above 420 nm are too low to exactly estimate the contributions), exhibiting large

272 day-night difference. For example, quinolines show evident absorption below 340 nm (3.6% at

273 310 nm during the day), but negligible contribution above 360 nm. Nitrophenols exhibit a

274 maximum contribution at about 350 nm, while nitrocatechols show higher absorption in the

275 wavelength range from 360 to 400 nm. For PAHs, the absorption maxima shift to a longer

276 wavelength with the increase of the aromatic rings (e.g., 320 nm for 4-ring PAHs and 400 nm

277 for 6-ring PAHs). Overall, the combined light absorption contributions of nitrophenols,

278 nitrocatechols, and PAHs are 86.5% and 80.1% (averaged between 300 and 420 nm) at night

279 and day, respectively. This result is similar to previous studies, in which PAHs and nitro

280 aromatic compounds were identified as the major chromophores (Huang et al., 2020; Yuan et

281 al., 2020).

282   The light absorption contribution of these BrC subgroups exhibits obvious day-night

283 differences. For example, the absorption contribution of 2–3-rings OPAHs and nitrocatechols

284 at 365 nm increased by ~2.0 and ~3.5 times during the day compared to that during the night

285 (see Figure S2). This result differs from previous studies (Kampf et al., 2012; Gao et al., 2022),

286 which indicated that light absorption of BrC compounds were enhanced after exposure to photo-

287 oxidation. On the other hand, the absorption contributions of nitrophenols and 4–6-rings PAHs

288 at 365 nm are ~1.6 times and ~2.2 times higher at night than at day, respectively. The day-night

289 difference of light absorption of nitrophenols is comparable with previous studies (Harrison et

290 al., 2005; Wang et al., 2020). High absorbance of nitrophenols at night is closely related to their

291 higher mass fraction at night. The absorption characteristics of 4–6-ring PAHs are significantly

292 different from the nitro-phenols, and their absorption per unit mass is larger than that of nitro-

293 phenols. The per unit mass absorbance of PAHs much higher than the low-ring aromatic

294 hydrocarbons (e.g., aromatic alcohols/acids) are due to their strongly conjugated systems. It is

295 worth noting that the absorption contributions of some BrC compounds (including quinolines,

Atmospheric
Chemistry
and Physics
Discussions
Open Access
EGU

296   aromatic alcohols/acids, 4-ring OPAHs, 3-ring PAHs four subgroups) are much lower than

297   those of the above-mentioned BrC compounds because of their lower mass concentration or

298   light absorption coefficient.

3.3 Comparisons between the low and high pollution period.

300   The relative contributions of day-night subgroups of BrC chromophores in light absorption

301   and mass concentration were further investigated for different pollution levels. The sampling

302   campaign was classified into low-pollution period ($PM_{2.5}$< 150 µg m^{-3}) and high-pollution

303   period ($PM_{2.5}$ >250 µg m^{-3}). Figure 4 (a) shows the mass fractional contributions of the

304   identified subgroups during these periods, which show an evidently different during the day

305   and night. For example, the mass fraction of quinolines during the day (~24.1%) is much higher

306   than during the night (3.4%) at low-pollution period, which may be related to increased vehicle

307   emissions at day (Rogge et al., 1993; Lyu et al., 2019). Moreover, during the low-pollution

308   period, with good atmospheric dispersion conditions during the day, the fractional concentration

309   of BrC is only 56.9 ng m^{-3} much lower than the nights and high-pollution periods. In the high-

310   pollution period, however, the mass concentration of quinolines is much lower than other BrC

311   chromophores and there is no evident difference between day and night. The mass fraction of

312   aromatic alcohols/acids during the day (35.4%) is much higher than during the night (12.0%)

313   at low-pollution period. For high-pollution period, the mass fraction of aromatic alcohols/acids

314   shows little difference between the day and night. However, their mass concentration during

315   the day (55.5 ng m^{-3}) is higher than that during the night (31.9 ng m^{-3}). Thereinto, the mass

316   concentration of phthalic acid (a tracer from photochemical oxidation) contributes more than

317   60% to the aromatic alcohols/acids at day for low and high-pollution period (Zhang and

318   Hatakeyama, 2016). This evidence may be suggesting that there is stronger photo-chemical

319   oxidation for aromatic alcohols/acids during the day, especially at low-pollution period.

320   The mass fractional contribution of nitrocatechols is lower during the day than the night

321   at low-pollution period, while there is obvious secondary formation during the day for high-

322   pollution period. This likely suggests that the daytime conditions of the high-pollution period

323   are inducive for the generation of nitrocatechols. The mass fractional contribution of PAHs

324   during the day is much lower than the night at low-pollution period. At night, residential coal

Atmospheric
Chemistry
and Physics
Discussions

Open Access

EGU

325 heating is an important source of PAHs, and therefore the daytime contributions of PAHs are

326 much lower than nighttime (Wang et al., 2017; Ni et al., 2021). While there is no day-night

327 difference for PAHs at high-pollution period, which is related to the stable sources and stagnant

328 weather conditions (Huang et al., 2019; Lin et al., 2020). It is noteworthy that the mass

329 contributions of the nitrophenols (nighttime is 2–3 times more than daytime) and 2–3-rings

330 OPAHs (daytime is ~2 times more than nighttime) is opposite between the day and night. This

331 demonstrates that they have stable sources compared to other BrC subgroups even during the

332 low-pollution period and high-pollution period. The higher mass fractional contribution of 2–

333 3-rings OPAHs during the day is related to photochemical oxidation. Nitrophenols exhibit a

334 higher mass fractional contribution during the night than the day, indicating a significant

335 contribution from primary emissions (Lu et al., 2019; Lin et al., 2020). Besides, previous

336 investigations have shown that NO_x concentrations and relative humidity are higher at night in

337 Shijiazhuang, which may have accelerated the formation of nitrophenols in the dark (Yuan et

338 al., 2016; Huang et al., 2019). This result exhibits a clear day-night difference during the low-

339 pollution period than high-pollution period, which indicates that the low-pollution period is

340 easily influenced by the external environment (e.g., solar radiation and wind speed).

341 The day-night light absorption contribution of WS-BrC and WIS-BrC chromophores in

342 different pollution periods is shown in Figure 4 (b). For the low-pollution period, the light

343 absorption contribution of the ten BrC subgroups shows a large difference during the day and

344 night. Thereinto, the WS-BrC chromophores (e.g., quinolines, nitrophenols and nitrocatechols)

345 is the main contributor (accounting for ~75% at 365 nm) of total identified BrC during the day.

346 While, the WIS-BrC chromophores (e.g., 4–6-rings PAHs) become an abundance contributor

347 (accounting for ~65% at 365 nm) during the night. There is an obvious day-night differences in

348 light absorption at low-pollution period, which is consistent with the difference in their mass

349 concentration contribution. Different from the low-pollution period, the light absorption

350 contribution of the total WS-BrC and WIS-BrC chromophores showed no significant day-night

351 differences during the high-pollution period. However, the absorption contributions of

352 subgroups in WS-BrC chromophores have a significant day-night difference (e.g., nitrocatechol

353 and nitrophenols) during the high-pollution period, which is due to the change of the mass

Atmospheric
Chemistry
and Physics
Discussions
Open Access
EGU

354   contributions. WS-BrC chromophores have stronger light absorption both during the day and

355   night compared to the WIS-BrC chromophores at high pollution period. Specifically, the

356   absorption contribution of nitrocatechols and nitrophenols combined accounts for 66.1% at day

357   and 60.7% at night at 365 nm, respectively, which depend on the different emission sources or

358   formation mechanisms between during the day and night. Our results show a significant day-

359   night differences in mass contributions and absorption contributions of BrC components at

360   different pollution levels. This suggests that the variation of BrC chromophores in different

361   pollution periods may be caused by different sources and weather conditions.

362   **4   Conclusions**

363   In general, our study shows the large day-night differences in optical properties and

364   chemical composition of the bulk BrC in urban atmosphere. Thereinto, WS-BrC is the main

365   light-absorbing contributors during the day, while WIS-BrC is main light-absorbing compound

366   at night. Different types of the identified BrC chromophores exhibit unique characteristics of

367   day-night differences, reflecting their particular sources and formation pathways. For example,

368   nitrocatechols and 2–3-rings OPAHs are important contributors to mass concentration and light

369   absorption during the day, while 4–6-rings PAHs and nitrophenols become the significant

370   contributors at night. Day-night differences of BrC chromophores are associated with different

371   sources during day (more secondary formation) and night (more primary emissions).

372   Moreover, these day-night differences are largely affected by the air pollution level, which

373   determines the concentrations of BrC precursors (e.g., aromatic hydrocarbon and phenols) and

374   oxidants (e.g., NO_x, $NO_3^{\cdot}$ and OH), as well as meteorological conditions (e.g., solar irradiation

375   and RH) (Liu et al., 2012; Laskin et al., 2015; Wang et al., 2019). For example, our results found

376   that the day-night difference of BrC fractions is more pronounced in chemical composition and

377   light absorption during the low-pollution period than high-pollution period. These factors may

378   show different effects on the formation and photobleaching of different types of the identified

379   chromophores. However, our current understanding of the formation mechanisms of and

380   influencing factors on these identified chromophores is still incomplete (Huang et al., 2018;

381   Yuan et al., 2020). Therefore, a combination of more laboratory and field studies is needed to

382   (1) make comprehensive characterization of the chromophore composition BrC in ambient

Atmospheric
Chemistry
and Physics
Discussions

Open Access

EGU

383 aerosol; (2) explore thoroughly the formation mechanisms of different types of BrC

384 chromophore. This will significantly enhance our understanding of atmospheric BrC formation

385 mechanisms and therefore improve the accuracy of the atmospheric effects of BrC in air quality

386 and climate models.

Atmospheric
Chemistry
and Physics
Discussions

Atmospheric
Chemistry
and Physics
Discussions

References

400 Alcanzare, R. J. C.: Polycyclic aromatic compounds in wood soot extracts from Henan, China, 2006.

402 Banerjee, S. and Zare, R. N.: Syntheses of isoquinoline and substituted quinolines in charged
403   microdroplets, Angew. Chem., 127, 15008-15012, 2015.

404 Chen, L.-W. A., Chow, J. C., Wang, X., Cao, J., Mao, J., and Watson, J. G.: Brownness of Organic
405   Aerosol over the United States: Evidence for Seasonal Biomass Burning and Photobleaching
406   Effects, Environ. Sci. Technol., 55, 8561-8572, 10.1021/acs.est.0c08706, 2021.

407 Chen, Y. and Bond, T. C.: Light absorption by organic carbon from wood combustion, Atmos. Chem.
408   Phys., 10, 1773-1787, 10.5194/acp-10-1773-2010, 2010.

409 Cheng, Y., He, K.-b., Du, Z.-y., Engling, G., Liu, J.-m., Ma, Y.-l., Zheng, M., and Weber, R. J.: The
410   characteristics of brown carbon aerosol during winter in Beijing, Atmos. Environ., 127, 355-364,
411   10.1016/j.atmosenv.2015.12.035, 2016.

412 Chow, J. C., Watson, J. G., Robles, J., Wang, X., Chen, L.-W. A., Trimble, D. L., Kohl, S. D., Tropp,
413   R. J., and Fung, K. K.: Quality assurance and quality control for thermal/optical analysis of
414   aerosol samples for organic and elemental carbon, Anal. Bioanal. Chem., 401, 3141-3152, 2011.

415 Chow, K. S., Huang, X. H., and Yu, J. Z.: Quantification of nitroaromatic compounds in atmospheric
416   fine particulate matter in Hong Kong over 3 years: field measurement evidence for secondary
417   formation derived from biomass burning emissions, Environ.Chem., 13, 665-673, 2015.

418 Dat, N. D. and Chang, M. B.: Review on characteristics of PAHs in atmosphere, anthropogenic
419   sources   and   control   technologies,   Sci   Total   Environ.,   609,   682-693,
420   10.1016/j.scitotenv.2017.07.204, 2017.

421 Deng, J., Ma, H., Wang, X., Zhong, S., Zhang, Z., Zhu, J., Fan, Y., Hu, W., Wu, L., Li, X., Ren, L.,
422   Pavuluri, C. M., Pan, X., Sun, Y., Wang, Z., Kawamura, K., and Fu, P.: Measurement report:
423   Optical properties and sources of water-soluble brown carbon in Tianjin, North China – insights
424   from organic molecular compositions, Atmos. Chem. Phys., 22, 6449-6470, 10.5194/acp-22-
425   6449-2022, 2022.

426 Gao, Y., Wang, Q., Li, L., Dai, W., Yu, J., Ding, L., Li, J., Xin, B., Ran, W., and Han, Y.: Optical
427   properties of mountain primary and secondary brown carbon aerosols in summertime, Sci Total
428   Environ., 806, 150570, 2022.

429 Hammer, M. S., Martin, R. V., van Donkelaar, A., Buchard, V., Torres, O., Ridley, D. A., and Spurr,
430   R. J. D.: Interpreting the ultraviolet aerosol index observed with the OMI satellite instrument to
431   understand absorption by organic aerosols: implications for atmospheric oxidation and direct
432   radiative effects, Atmos. Chem. Phys., 16, 2507-2523, 10.5194/acp-16-2507-2016, 2016.

433 Harrison, M. A., Barra, S., Borghesi, D., Vione, D., Arsene, C., and Olariu, R. I.: Nitrated phenols
434   in the atmosphere: a review, Atmos. Environ., 39, 231-248, 2005.

435 Hems, R. F. and Abbatt, J. P. D.: Aqueous Phase Photo-oxidation of Brown Carbon Nitrophenols:
436   Reaction Kinetics, Mechanism, and Evolution of Light Absorption, ACS Earth Space Chem., 2,
437   225-234, 10.1021/acsearthspacechem.7b00123, 2018.

438 Hecobian, A., Zhang, X., Zheng, M., Frank, N., Edgerton, E. S., and Weber, R. J.: Water-Soluble
439   Organic Aerosol material and the light-absorption characteristics of aqueous extracts measured
440   over the Southeastern United States, Atmos. Chem. Phys., 10, 5965-5977, 2010.

441 Huang, R.-J., Wang, Y., Cao, J., Lin, C., Duan, J., Chen, Q., Li, Y., Gu, Y., Yan, J., and Xu, W.:
442   Primary emissions versus secondary formation of fine particulate matter in the most polluted city
443   (Shijiazhuang) in North China, Atmos. Chem. Phys., 19, 2283-2298, 2019.

444   Huang, R.-J., Yang, L., Cao, J., Chen, Y., Chen, Q., Li, Y., Duan, J., Zhu, C., Dai, W., and Wang, K.:
445   Brown carbon aerosol in urban Xi'an, Northwest China: the composition and light absorption
446   properties, Environ. Sci. Technol., 52, 6825-6833, 2018.

447   Huang, R.-J., Yang, L., Shen, J., Yuan, W., Gong, Y., Ni, H., Duan, J., Yan, J., Huang, H., and You,
448   Q.: Chromophoric Fingerprinting of Brown Carbon from Residential Biomass Burning, Environ.
449   Sci. Technol. Lett., 2021.

450   Huang, R.-J., Zhang, Y., Bozzetti, C., Ho, K.-F., Cao, J.-J., Han, Y., Daellenbach, K. R., Slowik, J.
451   G., Platt, S. M., and Canonaco, F.: High secondary aerosol contribution to particulate pollution
452   during haze events in China, Nature, 514, 218-222, 2014.

453   Huang, R. J., Yang, L., Shen, J., Yuan, W., Gong, Y., Guo, J., Cao, W., Duan, J., Ni, H., Zhu, C., Dai,
454   W., Li, Y., Chen, Y., Chen, Q., Wu, Y., Zhang, R., Dusek, U., O'Dowd, C., and Hoffmann, T.:
455   Water-Insoluble Organics Dominate Brown Carbon in Wintertime Urban Aerosol of China:
456   Chemical   Characteristics and Optical Properties, Environ Sci Technol., 54, 7836-7847,
457   10.1021/acs.est.0c01149, 2020.

458   Iinuma, Y., Böge, O., Gräfe, R., and Herrmann, H.: Methyl-nitrocatechols: atmospheric tracer
459   compounds for biomass burning secondary organic aerosols, Environ Sci Technol., 44, 8453-
460   8459, 2010.

461   Kampf, C. J., Jakob, R., and Hoffmann, T.: Identification and characterization of aging products in
462   the glyoxal/ammonium sulfate system–implications for light-absorbing material in atmospheric
463   aerosols, Atmos. Chem. Phys., 12, 6323-6333, 2012.

464   Kasthuriarachchi, N. Y., Rivellini, L. H., Chen, X., Li, Y. J., and Lee, A. K. Y.: Effect of Relative
465   Humidity on Secondary Brown Carbon Formation in Aqueous Droplets, Environ Sci Technol.,
466   54, 13207-13216, 10.1021/acs.est.0c01239, 2020.

467   Kirchstetter, T. W., Novakov, T., and Hobbs, P. V.: Evidence that the spectral dependence of light
468   absorption by aerosols is affected by organic carbon, J Geophys Res-Atmos., 109, 2004.

469   Kitanovski, Z., Grgić, I., Yasmeen, F., Claeys, M., and Čusak, A.: Development of a liquid
470   chromatographic method based on ultraviolet–visible and electrospray ionization mass
471   spectrometric detection for the identification of nitrocatechols and related tracers in biomass
472   burning atmospheric organic aerosol, Rapid Commun Mass Sp., 26, 793-804, 2012.

473   Laskin, A., Laskin, J., and Nizkorodov, S. A.: Chemistry of atmospheric brown carbon, Chem Rev.,
474   115, 4335-4382, 10.1021/cr5006167, 2015.

475   Li, J., Zhang, Q., Wang, G., Li, J., Wu, C., Liu, L., Wang, J., Jiang, W., Li, L., and Ho, K. F.: Optical
476   properties and molecular compositions of water-soluble and water-insoluble brown carbon (BrC)
477   aerosols in northwest China, Atmos. Chem. Phys., 20, 4889-4904, 2020.

478   Li, X., Zhao, Q., Yang, Y., Zhao, Z., Liu, Z., Wen, T., Hu, B., Wang, Y., Wang, L., and Wang, G.:
479   Composition and sources of brown carbon aerosols in megacity Beijing during the winter of 2016,
480   Atmos. Res., 262, 105773, 2021.

481   Lin, C., Huang, R.-J., Xu, W., Duan, J., Zheng, Y., Chen, Q., Hu, W., Li, Y., Ni, H., and Wu, Y.:
482   Comprehensive Source Apportionment of Submicron Aerosol in Shijiazhuang, China: Secondary
483   Aerosol Formation and Holiday Effects, ACS Earth and Space Chem., 4, 947-957, 2020.

484   Lin, P., Bluvshtein, N., Rudich, Y., Nizkorodov, S. A., Laskin, J., and Laskin, A.: Molecular
485   Chemistry of Atmospheric Brown Carbon Inferred from a Nationwide Biomass Burning Event,
486   Environ. Sci. Technol., 51, 11561-11570, 10.1021/acs.est.7b02276, 2017.

487   Liu, S., Shilling, J. E., Song, C., Hiranuma, N., Zaveri, R. A., and Russell, L. M.: Hydrolysis of

488   organonitrate functional groups in aerosol particles, Aerosol. Sci. Technol., 46, 1359-1369, 2012.

489   Liu, J., Lin, P., Laskin, A., Laskin, J., Kathmann, S. M., Wise, M., Caylor, R., Imholt, F., Selimovic,
490   V., and Shilling, J. E.: Optical properties and aging of light-absorbing secondary organic aerosol,
491   Atmos. Chem. Phys., 16, 12815-12827, 10.5194/acp-16-12815-2016, 2016.

492   Liu, W.-J., Li, W.-W., Jiang, H., and Yu, H.-Q.: Fates of chemical elements in biomass during its
493   pyrolysis, Chem. Rev., 117, 6367-6398, 2017.

494   Lu, C., Wang, X., Li, R., Gu, R., Zhang, Y., Li, W., Gao, R., Chen, B., Xue, L., and Wang, W.:
495   Emissions of fine particulate nitrated phenols from residential coal combustion in China, Atmos.
496   Environ., 203, 10-17, https://doi.org/10.1016/j.atmosenv.2019.01.047, 2019.

497   Lyu, R., Shi, Z., Alam, M. S., Wu, X., Liu, D., Vu, T. V., Stark, C., Fu, P., Feng, Y., and Harrison, R.
498   M.: Insight into the composition of organic compounds ($\geq$ C 6) in PM 2.5 in wintertime in Beijing,
499   China, Atmos. Chem. Phys., 19, 10865-10881, 2019.

500   Ni, H., Huang, R.-J., Pieber, S. M., Corbin, J. C., Stefenelli, G., Pospisilova, V., Klein, F., Gysel-
501   Beer, M., Yang, L., and Baltensperger, U.: Brown carbon in primary and aged coal combustion
502   emission, Environ. Sci. Technol., 55, 5701-5710, 2021.

503   Rogge, W. F., Hildemann, L. M., Mazurek, M. A., Cass, G. R., and Simoneit, B. R.: Sources of fine
504   organic aerosol. 2. Noncatalyst and catalyst-equipped automobiles and heavy-duty diesel trucks,
505   Environ. Sci. Technol., 27, 636-651, 1993.

506   Scaramboni, C., Urban, R. C., Lima-Souza, M., Nogueira, R. F. P., Cardoso, A. A., Allen, A. G., and
507   Campos, M. d. M.: Total sugars in atmospheric aerosols: An alternative tracer for biomass burning,
508   Atmos. Environ., 100, 185-192, 2015.

509   Schnitzler, E. G. and Abbatt, J. P.: Heterogeneous OH oxidation of secondary brown carbon aerosol,
510   Atmos. Chem. Phys., 18, 14539-14553, 2018.

511   Shen, R., Liu, Z., Chen, X., Wang, Y., Wang, L., Liu, Y., and Li, X.: Atmospheric levels, variations,
512   sources and health risk of PM2. 5-bound polycyclic aromatic hydrocarbons during winter over
513   the North China Plain, Sci. Total Environ., 655, 581-590, 2019.

514   Siemens, K., Morales, A., He, Q., Li, C., Hettiyadura, A. P., Rudich, Y., and Laskin, A.: Molecular
515   Analysis of Secondary Brown Carbon Produced from the Photooxidation of Naphthalene,
516   Environ. Sci. Technol., 56, 3340-3353, 2022.

517   Teich, M., van Pinxteren, D., Wang, M., Kecorius, S., Wang, Z., Müller, T., Močnik, G., and
518   Herrmann, H.: Contributions of nitrated aromatic compounds to the light absorption of water-
519   soluble and particulate brown carbon in different atmospheric environments in Germany and
520   China, Atmos. Chem. Phys., 17, 1653-1672, 2017.

521   Wang, H., Gao, Y., Wang, S., Wu, X., Liu, Y., Li, X., Huang, D., Lou, S., Wu, Z., and Guo, S.:
522   Atmospheric processing of nitrophenols and nitrocresols from biomass burning emissions, J.
523   Geophys.Res. Atmos., 125, e2020JD033401, 2020.

524   Wang, L., Wang, X., Gu, R., Wang, H., Yao, L., Wen, L., Zhu, F., Wang, W., Xue, L., Yang, L., Lu,
525   K., Chen, J., Wang, T., Zhang, Y., and Wang, W.: Observations of fine particulate nitrated phenols
526   in four sites in northern China: concentrations, source apportionment, and secondary formation,
527   Atmos. Chem. Phys., 18, 4349-4359, 10.5194/acp-18-4349-2018, 2018.

528   Wang, Q., Han, Y., Ye, J., Liu, S., Pongpiachan, S., Zhang, N., Han, Y., Tian, J., Wu, C., and Long,
529   X.: High contribution of secondary brown carbon to aerosol light absorption in the southeastern
530   margin of Tibetan Plateau, Geophys.Res. Lett., 46, 4962-4970, 2019a.

531   Wang, X., Gu, R., Wang, L., Xu, W., Zhang, Y., Chen, B., Li, W., Xue, L., Chen, J., and Wang, W.:

532   Emissions of fine particulate nitrated phenols from the burning of five common types of biomass,
533   Environ Pollut., 230, 405-412, 10.1016/j.envpol.2017.06.072, 2017.

534   Wang, Y., Hu, M., Wang, Y., Zheng, J., Shang, D., Yang, Y., Liu, Y., Li, X., Tang, R., and Zhu, W.:
535   The formation of nitro-aromatic compounds under high NO x and anthropogenic VOC conditions
536   in urban Beijing, China, Atmos. Chem. Phys., 19, 7649-7665, 2019b.

537   Xie, C., Xu, W., Wang, J., Wang, Q., Liu, D., Tang, G., Chen, P., Du, W., Zhao, J., and Zhang, Y.:
538   Vertical characterization of aerosol optical properties and brown carbon in winter in urban Beijing,
539   China, Atmos. Chem. Phys., 19, 165-179, 2019.

540   Xue, X., Zeng, M., and Wang, Y.: Highly active and recyclable Pt nanocatalyst for hydrogenation
541   of quinolines and isoquinolines, Applied Catalysis A: General., 560, 37-41, 2018.

542   Yuan, B., Liggio, J., Wentzell, J., Li, S.-M., Stark, H., Roberts, J. M., Gilman, J., Lerner, B., Warneke,
543   C., and Li, R.: Secondary formation of nitrated phenols: insights from observations during the
544   Uintah Basin Winter Ozone Study (UBWOS) 2014, Atmos. Chem. Phys., 16, 2139-2153, 2016.

545   Yuan, W., Huang, R.-J., Yang, L., Guo, J., Chen, Z., Duan, J., Wang, T., Ni, H., Han, Y., and Li, Y.:
546   Characterization of the light-absorbing properties, chromophore composition and sources of
547   brown carbon aerosol in Xi'an, northwestern China, Atmos. Chem. Phys., 20, 5129-5144, 2020.

548   Yuan, W., Huang, R.-J., Yang, L., Wang, T., Duan, J., Guo, J., Ni, H., Chen, Y., Chen, Q., and Li, Y.:
549   Measurement report: PM 2.5-bound nitrated aromatic compounds in Xi'an, Northwest China–
550   seasonal variations and contributions to optical properties of brown carbon, Atmos. Chem. Phys.,
551   21, 3685-3697, 2021.

552   Zhan, Y., Li, J., Tsona, N. T., Chen, B., Yan, C., George, C., and Du, L.: Seasonal variation of water-
553   soluble brown carbon in Qingdao, China: Impacts from marine and terrestrial emissions, Environ.
554   Res., 212, 113144, https://doi.org/10.1016/j.envres.2022.113144, 2022.

555   Zhang, S., Zhang, W., Wang, K., Shen, Y., Hu, L., and Wang, X.: Concentration, distribution and
556   source apportionment of atmospheric polycyclic aromatic hydrocarbons in the southeast suburb
557   of Beijing, China, Environ. Monit. Assess., 151, 197-207, 2009.

558   Zhang, Y. and Hatakeyama, S.: New directions: Need for better understanding of source and
559   formation process of phthalic acid in aerosols as inferred from, Atmos. Environ., 140, 147e149,
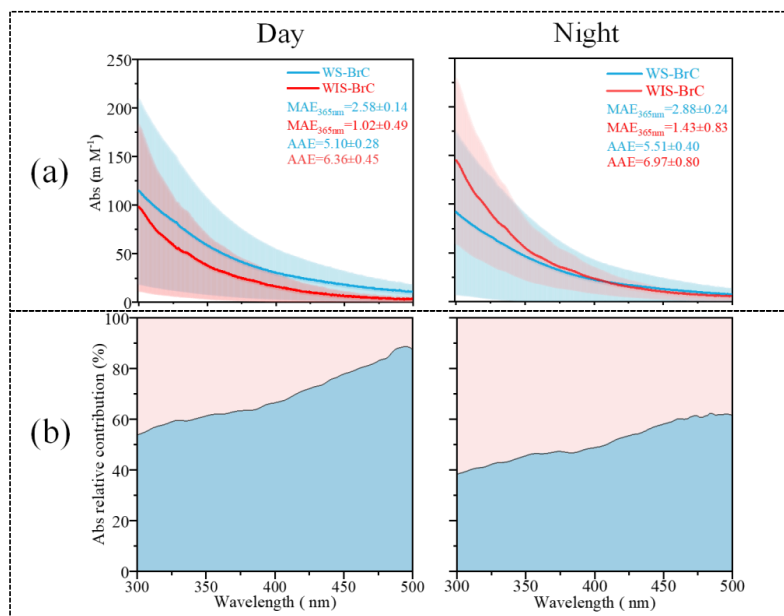560   2016.

Figure 1. (a) Day-night absorption spectra (Abs, in the wavelength range of 300–500 nm), mass absorption efficiency (MAE, determined at 365 nm), and absorption Ångström exponent (AAE, calculated between 300 and 400 nm) of water-soluble/insoluble BrC (WS-/WIS-BrC) in Shijiazhuang. (b) Light-absorbing proportion of WS-BrC and WIS-BrC between 300 to 500 nm.
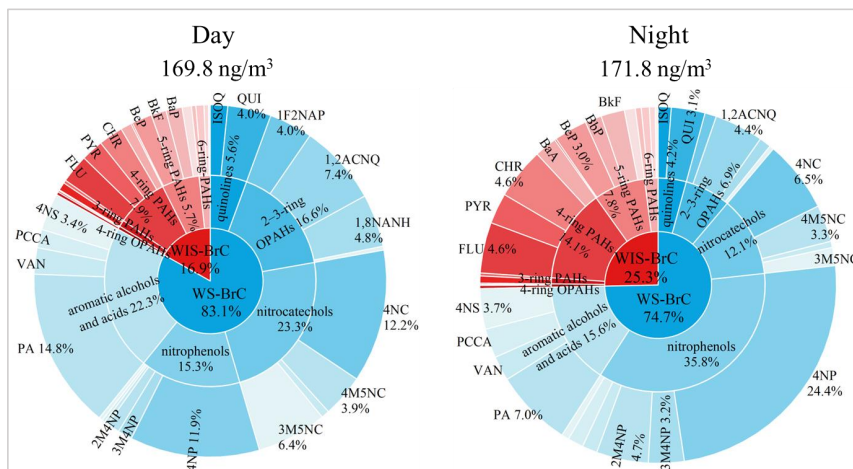

Figure 2. Mass fraction of the identified BrC chromophores during the day and night (details of the identified BrC chromophores are shown in Table S1).
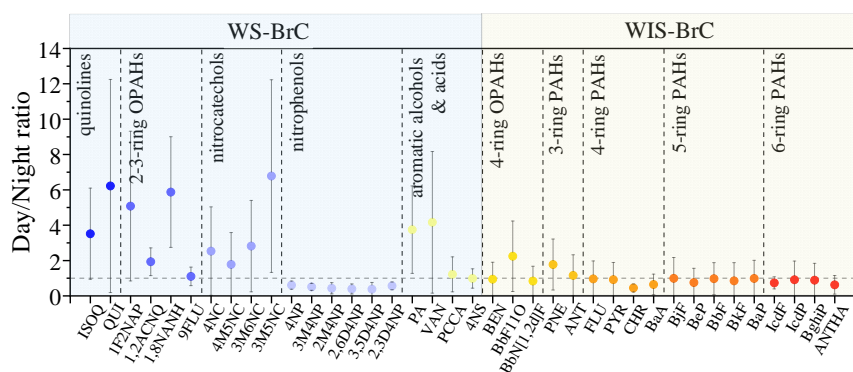
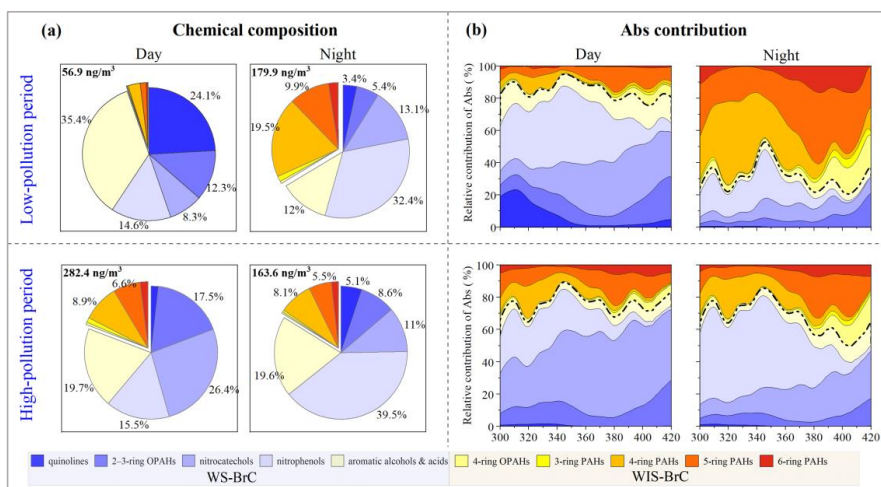**Figure 3**. Day-to-night ratios of the concentrations of different BrC chromophores.

Figure 4. Day-night fractional contributions of mass concentrations **(a)** and light absorption **(b)** of the ten BrC subgroups in low-pollution period and high-pollution period. Here the BrC chromophore is the main chromophore substance that has been identified. In **(b)** WS-BrC is below the dotted line and WIS-BrC is above the dotted line.